Equivalence of chain conformations in the surface region of a polymer melt and a single Gaussian chain under critical conditions

ARTICLE *in* THE JOURNAL OF CHEMICAL PHYSICS · AUGUST 2013

Impact Factor: 2.95 · DOI: 10.1063/1.4817339 · Source: PubMed

3 AUTHORS:

Alexander M. Skvortsov
Chemical Pharmaceutical Academie . St.Pete…
152 PUBLICATIONS **1,670** CITATIONS
SEE PROFILE

Frans A M Leermakers
Wageningen University
288 PUBLICATIONS **4,741** CITATIONS
SEE PROFILE

Gerard J Fleer
Wageningen University
206 PUBLICATIONS **8,242** CITATIONS
SEE PROFILE

Equivalence of chain conformations in the surface region of a polymer melt and a single Gaussian chain under critical conditions

A. M. Skvortsov, F. A. M. Leermakers, and G. J. Fleer

Citation: J. Chem. Phys. **139**, 054907 (2013); doi: 10.1063/1.4817339
View online: http://dx.doi.org/10.1063/1.4817339
View Table of Contents: http://jcp.aip.org/resource/1/JCPSA6/v139/i5
Published by the AIP Publishing LLC.

Equivalence of chain conformations in the surface region of a polymer melt and a single Gaussian chain under critical conditions

A. M. Skvortsov,[1] F. A. M. Leermakers,[2] and G. J. Fleer[2]
[1]*Chemical Pharmaceutical Academy, Prof. Popova 14, 197022 St Petersburg, Russia*
[2]*Laboratory of Physical Chemistry and Colloid Science, Wageningen University, Dreijenplein 6, 6703 HB Wageningen, The Netherlands*

(Received 7 May 2013; accepted 19 July 2013; published online 7 August 2013)

In the melt polymer conformations are nearly ideal according to Flory's ideality hypothesis. Silberberg generalized this statement for chains in the interfacial region. We check the Silberberg argument by analyzing the conformations of a probe chain end-grafted at a solid surface in a sea of floating free chains of concentration φ by the self-consistent field (SCF) method. Apart from the grafting, probe chain and floating chains are identical. Most of the results were obtained for a standard SCF model with freely jointed chains on a six-choice lattice, where immediate step reversals are allowed. A few data were generated for a five-choice lattice, where such step reversals are forbidden. These coarse-grained models describe the equilibrium properties of flexible atactic polymer chains at the scale of the segment length. The concentration was varied over the whole range from $\varphi = 0$ (single grafted chain) to $\varphi = 1$ (probe chain in the melt). The number of contacts with the surface, average height of the free end and its dispersion, average loop and train length, tail size distribution, end-point and overall segment distributions were calculated for a grafted probe chain as a function of φ, for several chain lengths and substrate/polymer interactions, which were varied from strong repulsion to strong adsorption. The computations show that the conformations of the probe chain in the melt do not depend on substrate/polymer interactions and are very similar to the conformations of a single end-grafted chain under critical conditions, and can thus be described analytically. When the substrate/polymer interaction is fixed at the value corresponding to critical conditions, all equilibrium properties of a probe chain are independent of φ, over the whole range from a dilute solution to the melt. We believe that the conformations of all flexible chains in the surface region of the melt are close to those of an appropriate single chain in critical conditions, provided that one end of the single chain is fixed at the same point as a chain in the melt. [http://dx.doi.org/10.1063/1.4817339]

I. INTRODUCTION

The conformations of a polymer chain near a solid substrate at different concentrations are not only interesting from a fundamental point of view but are also important for various applications, e.g., in coatings, lubricants, and composite materials, where these macromolecules control the overall performance of such systems. The presence of a solid boundary introduces deviations in both the structural and dynamic properties as compared to those in the bulk (solution). The extent of this perturbation is generally not well understood at the molecular level. In this sense, computer simulations for studying the polymer conformations have proved to be quite useful, because the structure can be studied in detail.

Examples of such atomistic simulations are those of Yelash *et al.*[1] (graphite/polybutadiene), Hentsche *et al.*[2] (graphite/alkane), Mansfield and Theodorou[3] (vacuum/atactic polypropylene), Smith *et al.*[4] (atomistic surface/n-alkane), Daoulas *et al.*[5] (graphite/polyethylene), and Pandey and Doxastakis[6] (silica/polyethylene). They give a lot of atomistic information, as long as the concentrations are not too high. When the concentration approaches the conditions of a polymer melt, these simulations suffer from the problem that most of the moves have to be rejected, so that the statistics become unreliable.

As an alternative strategy one can use coarse-grained models, either on a mean-field level (Scheutjens *et al.*,[7,8] Muller *et al.*,[9] Theodorou[10]) or Monte-Carlo or Molecular Dynamic simulations (Bitzanis *et al.*,[11,12] Smith *et al.*,[13] Ozmusul *et al.*,[14] Vacatello,[15] Meth and Lustig,[16] De Virgiliis *et al.*[17]). Then the substrate has no atomistic detail but is taken as a plane solid surface. In these coarse-grained models, the information obtained is necessarily less detailed. For the simulations, there are still problems to reach real melt conditions. However, the mean-field self-consistent field (SCF) model, based upon solving a (large) set of simultaneous equations, can easily find solutions for the melt.

There are conflicting conclusions about the properties of a polymer melt near a solid substrate. Many authors[5,6,10,17] believe that the conformational distortions in the melt depend on the adhesive strength of the substrate. They assume that the properties of the polymer-solid interface affect the conformations of the adsorbed chains. According to these expectations, controlling the adhesive strength of the polymer/solid interface is of crucial importance for the design of high-performance polymer-solid composite materials.

Therefore, proper definition of the polymer/substrate interaction potential is important in this type of calculations.

Other authors[9,11,12,18,19] follow the Silberberg[20] arguments that in the melt the chain conformations can be described as random walks with reflecting boundary conditions, and thus are similar to the conformations of a single chain under critical conditions. The melt, therefore, should show universal properties.

We adhere to the second group. We demonstrate that the melt has universal properties by calculating by SCF methods the conformations of an end-grafted probe chain in a solution of floating free chains of concentration φ, and we vary φ over the whole range from $\varphi = 0$ (single grafted chain in an athermal solvent, for which there are well-known analytical descriptions[21] available) to $\varphi = 1$ (one probe chain in the melt). Apart from the grafting, probe chain and floating chains are identical. We shall see that the conformations of the probe chain in the melt are very similar to those of a single end-grafted chain under critical conditions. Therefore, attractive or repulsive segment-surface interactions do not matter in the melt, and the melt conformations are indeed universal. Moreover, we have now an accurate analytical description of the probe chain conformations in the melt.

This paper is organized as follows. In Sec. II we describe the models used. Sections III and IV discuss concentration profiles, both of the floating chains (Sec. III) and of the probe chain (Sec. IV); in the latter case we consider both the distribution of end points and the overall distribution. Section V gives some noteworthy detail on the tail-length distribution. In Sec. VI we present some information about the train fraction and the average loop size. All the results of Secs. III–VI were obtained for a standard SCF model with a six-choice lattice. In Sec. VII we extend the treatment somewhat and give a few results for two more refined models: a five-choice lattice where immediate step reversals are forbidden and a Flory chain with internal excluded volume (then an isolated chain is swollen, but in the melt the chain is nearly Gaussian). In the discussion (Sec. VIII) we investigate some minor differences between the single chain at critical conditions and the probe chain in the melt; these differences are related to the potential profile, which is a pure square-well for a single chain at critical conditions, but shows typical (weak) oscillations in the melt. Finally, in the Appendix we show that the average tail length (and its dispersion) in SCF and in the analytical model for a Gaussian chain under critical conditions (and in the melt) are very close, but in SCF there are (small) finite chain-length corrections not present in the analytical model, which neglects the finite segment size.

II. MODEL

Most of the results presented in this paper were obtained for the simplest possible SCF model[7,8]: flexible freely jointed chains on a six-choice lattice, where the radius of gyration R of a free chain with N segments equals $\sqrt{(N/6)}$. The potential describing the interaction of the polymer segments with the solid surface has a standard rectangular form, with width equal to the segment size and depth or height χ_s. For attraction (depth) χ_s is negative, for repulsion (height) it is positive. We consider a probe chain which is end-grafted at the surface in a solution of floating non-grafted chains with bulk volume fraction φ and a monomeric solvent with bulk volume fraction $1 - \varphi$. The parameter φ is varied from 0 (one probe chain in solvent) to 1 (one probe chain in the melt). Probe chain and floating chains are identical (apart from the grafting): same chain length and same interaction parameters with solvent and surface. For simplicity we take the Flory-Huggins[22] polymer-solvent interaction parameter χ as zero, and we vary the polymer-surface interaction parameter χ_s to cover both repulsive and attractive interactions. An important reference is the critical point, where $\chi_s = \chi_{sc} = \ln(5/6)$ for a six-choice lattice. We use the parameter $\Delta\chi_s = \chi_s - \chi_{sc}$, which is positive for depletion, zero for critical conditions, and negative for adsorption.

For $\varphi = 0$ we shall compare the numerical SCF results with well-known analytical solutions[21] from a continuum model for a single grafted Gaussian chain, based upon the Edwards equation for zero field.[23,24] We shall use the analytical solution for two cases: strong repulsion and critical conditions (corresponding to weak segment-surface attraction, $\chi_{sc} = -0.182$). For strong attraction the analytical continuum theory cannot describe the SCF data because the volume-filling effect,[8,25] which then plays an dominating role and makes the field nonzero, is not accounted for.

The central issue in this paper is that, upon varying the volume fraction φ of the floating chains from 0 to 1, all the properties of the probe chain in the melt ($\varphi = 1$) converge to those of a single Gaussian chain ($\varphi = 0$) under critical conditions, for which we have an accurate analytical description. This convergence is *independent* of the polymer-surface interaction. We demonstrate this in the simple six-choice model for concentration profiles, end-point distributions, tail and loop length, and train fraction.

It is clear that a six-choice lattice and a continuum model for a Gaussian chain are only a rough approximation for a real polymer chain and a real polymer melt. In order to show that our basic assumption (melt conformations at $\varphi = 1$ equivalent to critical conformations at $\varphi = 0$) also holds for a slightly more sophisticated model, we present some data for a five-choice lattice, where immediate step reversals are forbidden. In this five-choice model $\chi_{sc} = \ln(4/5)$[26] (as compared to $\ln(5/6)$ for six-choice), and the radius of gyration is $R = \sqrt{(N/4)}$[26] (as compared to $\sqrt{(N/6)}$ for six-choice). We shall see that our basic assumption is also correct in this more refined model.

Both the six-choice and the five-choice lattice are typical mean-field models, in which a single chain does not swell because the field is zero: there is no internal excluded volume and $R \sim N^{0.5}$. Therefore, the SCF results for $\varphi = 0$ are close to analytical results for a Gaussian chain. It is possible to improve on that and use a more sophisticated SCF model which accounts for the internal excluded volume. In this approach the key ingredient is that we solve the SCF equations for an end-grafted chain on the surface in a two-gradient cylindrical coordinate system. We normalize the distribution of the grafted chain such that there are exactly N segments in this grafted chain. As a result the chain feels its intra-molecular excluded volume and swells accordingly. For

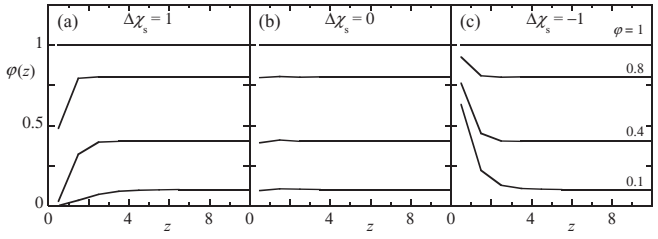

FIG. 1. Concentration profiles of the floating chains for (a) repulsion, $\Delta\chi_s = 1$, (b) critical conditions, $\Delta\chi_s = 0$, and (c) attraction, $\Delta\chi_s = -1$. The chain length is $N = 1000$, the bulk concentrations are $\varphi = 0.1$, 0.4, 0.8, and 1.

example, the non-adsorbing chain assumes a mushroom conformation with a radius proportional to $N^{0.6}$ in a good solvent. For the strongly adsorbing case the chain becomes a two-dimensional pancake with lateral size proportional to $N^{0.75}$. These are well-known results due to Flory[22] and, therefore, we refer to this case as the Flory-chain. Next, we consider the same two-gradient cylindrical coordinate system in the presence of a solution with freely floating polymers. We now get a Flory-chain which is swollen at $\varphi = 0$, but is again more or less Gaussian in the melt.

III. CONCENTRATION PROFILES OF THE FLOATING CHAINS

We start with a simple example: the concentration profile of the floating chains, for $N = 1000$ and $\varphi = 0.1$, 0.4, 0.8, and 1. Figure 1(a) is for repulsion ($\Delta\chi_s = 1$), Fig. 1(b) is for critical conditions ($\Delta\chi_s = 0$), and Fig. 1(c) is for attraction ($\Delta\chi_s = -1$). Such profiles have been reported many times before, so we do not analyze them in detail.

We only mention that in the repulsive regime the profiles can be approximated[27,28] as $\varphi(z) = \varphi \tanh^2[(z + p)/d]$, where p is the proximal length and d is the distal (decay) length. For very dilute solutions (not shown in Fig. 1(a)) p is small and depends only on χ_s, and $d = (2/\sqrt{\pi})R$ is close to the radius of gyration R. For the relation $p(\chi_s)$ we refer to the original literature.[25,28] For higher φ, as in Fig. 1(a), d is smaller and depends on φ; in semidilute and concentrated solutions d is roughly the correlation length $\xi \sim \varphi^{-1/2}$ (in a mean-field approximation). Clearly, in the melt $\varphi(z) = \varphi = 1$ for any z.

For attraction and φ above the overlap concentration $\varphi^* \approx 0.11$ (Fig. 1(c)), a reasonable approximation[27,29] is $\varphi(z) = \varphi \coth^2[(z + p)/d]$, with again $d \approx \xi$. In very dilute solutions (not shown in Fig. 1(c)) a different form[29] applies: $\varphi(z) \sim 1/\sinh^2[(z + p)/d]$, where d is now considerably smaller than R. For further details we refer to the original literature.[29]

In the critical point (Fig. 1(b)) the concentration profiles are essentially flat: $\varphi(z) = \varphi$. In this point the weak attraction ($\chi_s = \ln(5/6) = -0.182$) compensates the entropy loss of the polymer chains in the surface region and the probability to find a chain at some distance z from the surface does not depend on z. At the critical point the surface is "invisible" and "reflective boundary conditions" apply.[20]

The description of the concentration profiles near a repulsive solid surface is important for stabilization of colloids.[30] Most work focuses on the width of the depletion region, but not on the conformations of the polymer chain within it. In Secs. IV–VI we zoom in on the conformations of an end-grafted chain.

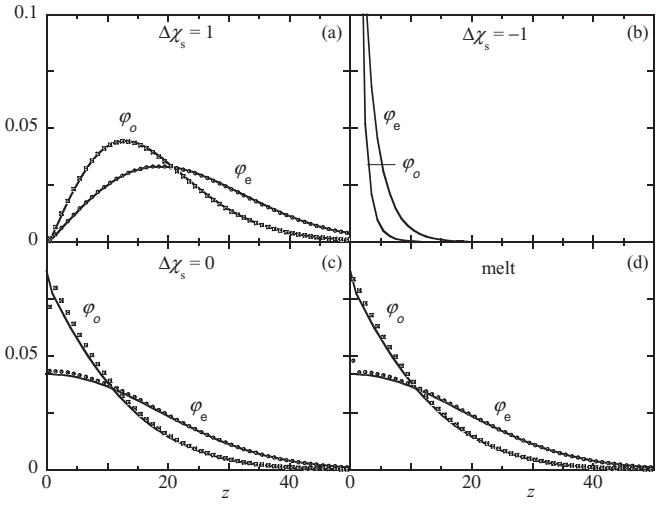

FIG. 2. End-point profiles $\varphi_e(z)$ and overall segment distribution $\varphi_o(z)$ of the probe chain ($N = 1000$). Diagrams (a), (b), (c) are for $\varphi = 0$ and (a) repulsion, $\Delta\chi_s = 1$, (b) attraction, $\Delta\chi_s = -1$, and (c) critical, $\Delta\chi_s = 0$. Diagram (d) is for the melt ($\varphi = 1$), where there is no effect of χ_s. In diagrams (a), (c), (d) the SCF results (symbols) are compared with analytical predictions (solid curves, see Eqs. (1) and (2)); those in (d) are copied from (c).

IV. END-POINT AND OVERALL SEGMENT DISTRIBUTION OF THE PROBE CHAIN

Figure 2 gives the SCF concentration profiles of the grafted probe chain, both the end-point distribution $\varphi_e(z)$ and the overall distribution $\varphi_o(z)$. All profiles are normalized to unity.

We compare the SCF results for $\varphi = 0$ (and $\varphi = 1$) with well-known analytical solutions[21] obtained from the continuum model for a single end-attached chain. These equations are most easily expressed in the parameter $\zeta = z/2R$, with $\zeta \geq 0$. For strong repulsion we have the following profiles, which are again normalized to unity:

$$\varphi_e(z) = \frac{1}{R}\zeta \exp(-\zeta^2), \tag{1a}$$

$$\varphi_o(z) = \frac{\sqrt{\pi}}{R}\left[\operatorname{erfc}(\zeta) - \operatorname{erfc}(2\zeta)\right]. \tag{1b}$$

For critical conditions the normalized analytical results are

$$\varphi_e(z) = \frac{1}{R\sqrt{\pi}} \exp(-\zeta^2), \tag{2a}$$

$$\varphi_o(z) = \frac{2}{R\sqrt{\pi}}[\exp(-\zeta^2) - \sqrt{\pi}\,\zeta \operatorname{erfc}(\zeta)]. \tag{2b}$$

Figure 2(a) is for $\varphi = 0$ and strong repulsion, where the conformation is like a mushroom. The SCF data are perfectly described by Eq. (1). As expected, the end-point profile is shifted further outwards than the overall profile. For the strongly attractive case and $\varphi = 0$ (Fig. 2(b)), where the

probe chain lies nearly flat (pancake), we have no easy analytical description because the volume filling is not accounted for, as mentioned in Sec. II. For a single chain at the critical point (Fig. 2(c)), there is again nice agreement between SCF and Eq. (2).

The most important feature of Fig. 2 is that the profiles of the probe chain in the melt (Fig. 2(d)) for any $\Delta\chi_s$ (from strong repulsion to strong attraction) are essentially the same as those for a single chain at critical conditions (Fig. 2(c)). As follows from Figs. 2(a) and 2(d), the mushroom conformations of the single chain grafted to a repulsive surface changes in the melt to the conformations of (half) a free Gaussian chain. The pancake conformations of the single chain at an attractive surface (Fig. 2(b)) transform in the melt to the same half-Gaussian conformations. These transformations illustrate Silberberg's argument: the chain conformations in the melt can be described as random walks reflected at the surface.

Upon close inspection, the SCF profile for φ_o of a single chain (Fig. 2(c)) and that for φ_e of the probe chain in the melt (Fig. 2(d)) show small jumps in the first layer ($z = 1/2$). These are related to the nonzero SCF field in the first layer; we return to these jumps in Sec. VIII.

In Fig. 2 we presented the end-point distribution for the two extremes: single chain at $\varphi = 0$ ($\Delta\chi_s = -1$, 0, 1) and the probe chain in the melt at $\varphi = 1$ (no effect of χ_s). It is interesting to see how this distribution develops when we gradually vary the bulk concentration φ from 0 to 1. Instead of giving the full profile for any φ, we shall discuss only some characteristics of the profiles: the 1st moment $z_1 = \langle z\rangle$, which is the average height of the end point, and the 2nd moment $z_2 = \langle z^2\rangle$. When the profiles are normalized to unity, as in Fig. 2 and Eqs. (1) and (2), these moments are defined as

$$z_1 = \langle z\rangle = \sum_{z=1/2}^{N-1/2} z\varphi_e(z), \tag{3a}$$

$$z_2 = \langle z^2\rangle = \sum_{z=1/2}^{N-1/2} z^2\varphi_e(z). \tag{3b}$$

The summation over $z = 0.5, 1.5, \ldots, N - 0.5$ is appropriate for the lattice model with finite segment size, where $z = 0.5$ is the middle of the train layer adjoining the surface. In the continuum model, where the finite segment size is disregarded, we replace the summation in Eq. (3) by an integral from 0 to N, and for long chains the upper integration limit may be taken as ∞.

Figure 3(a) gives the relative end-point position $\zeta_1 = z_1/2R$ for $N = 1000$ as a function of φ, for repulsion ($\Delta\chi_s = 2$ and 1), critical ($\Delta\chi_s = 0$), and attraction ($\Delta\chi_s = -1$ and -2). We first discuss the values for $\varphi = 0$, where for critical and repulsive conditions we can compare the SCF results with the analytical theory.

For strong attraction at $\varphi = 0$ the grafted probe chain lies nearly flat (pancake), and the average height of the free end $z_1 = \langle z\rangle$ is small and independent of N. SCF gives $z_1 = 1.835$, $\zeta_1 = 0.071$ for $\Delta\chi_s = -2$. For critical conditions z_1 is proportional to $\sqrt{N}$: the chain is weakly adsorbed

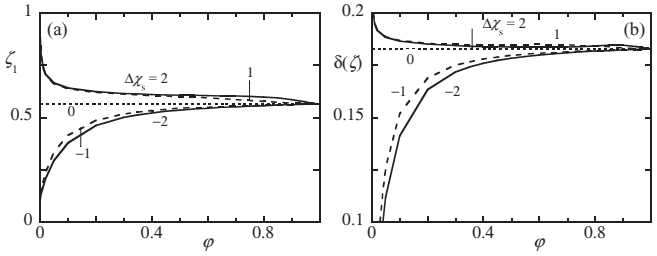

FIG. 3. The relative average height $\zeta_1 = z_1/2R = \langle z/2R\rangle$ of the free end of the grafted probe chain (a) and it dispersion $\delta(\zeta) = \delta(z/2R)$ (b) as a function of the bulk concentration φ of the floating chains, for $N = 1000$ and five values of $\Delta\chi_s$: 2, 1, 0, −1, −2.

and the end-point distribution is like that of (half) a Gaussian for a free chain. Equations (2a) and (3a) lead to the analytical result $\zeta_1 = \pi^{-1/2} = 0.564$, where now ζ_1 is independent of N. In SCF the data are nearly the same: $\zeta_1 = 0.567$. For repulsion the chain is more extended (mushroom): Eqs. (1a) and (3a) give the analytical result $\zeta_1 = \pi^{1/2}/2 = 0.886$, close to the SCF data ($\zeta_1 = 0.906$ for $\Delta\chi_s = 2$).

As the concentration φ of the floating chains increases, the average height ζ_1 of the free end for repulsion decreases very quickly, to reach a value in the melt which is nearly equal to that of a single chain at critical conditions. The average end-to-end distance normal to surface for a grafted chain in the melt is half the value of a free chain in the bulk. This reduction in the end-to-end distance was noted before,[15,16] without explanations.

For attraction there is a very steep increase of the end-to-end distance normal to surface. However, for critical conditions ζ_1 remains essentially constant over the entire concentration range. The SCF value for $\Delta\chi_s = 0$ and $\varphi = 1$ is $\zeta_1 = 0.564$, virtually the same value as for $\varphi = 0$. This independence of concentration φ for critical conditions is a very important feature, which applies not only to the average height but to all properties of the probe chain. It demonstrates that our basic concept (melt at $\varphi = 1$ equivalent to critical at $\varphi = 0$) holds. The fact that in the melt the parameter χ_s plays no role is also nicely shown by the convergence of the attractive and repulsive curves for high φ.

In Fig. 3(b) we plot the dispersion of ζ, defined as $\delta(\zeta) = \zeta_2 - {\zeta_1}^2 = z_2/4R^2 - (z_1/2R)^2 = \delta(z/2R)$. We see the same features as in Fig. 3(a): at $\varphi = 0$, $\delta(\zeta)$ is small for attraction and high for repulsion, but for high φ the attraction and repulsion curves converge to the critical value 0.183, which nicely agrees with the analytical value $1/2 - 1/\pi = 0.182$ from Eq. (2a).

V. TAIL LENGTH DISTRIBUTION

We start with an analytical result for a single grafted chain. Gorbunov *et al.*[31,32] derived the exact expression for the tail length distribution $n(s)$ of a grafted Gaussian chain at any N and any segment-surface interaction; here, $n(s)$ is the number of tails with length s. For strong attraction the chain has no long tails and $n(s)$ condenses to the region $s \ll N$ (see the curve for $\varphi = 0$ in Fig. 4(c)). For strong repulsion we find only long tails: $n(s) = 0$ for small s (see the curve for

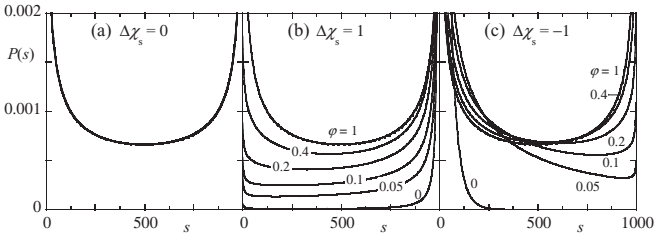

FIG. 4. Tail length distribution $P(s)$ of the probe chain for $N = 1000$ and six concentrations ($\varphi = 0$, 0.05, 0.1, 0.2, 0.4, 1) of the floating chains. Diagram (a) is for $\Delta\chi_s = 0$, where the distribution is symmetrical and independent of φ. In diagram (b) $\Delta\chi_s = 1$, in diagram (c) $\Delta\chi_s = -1$. All profiles are normalized to unity. The analytical result for the critical tail-length distribution is shown in all three diagrams as the dotted line; it essentially coincides with the melt data for any χ_s.

$\varphi = 0$ in Fig. 4(b)). We do not give the analytical (rather complicated) results for these cases, which have been shown to agree with SCF calculations,[32] but restrict ourselves here to critical conditions ($\Delta\chi_s = 0$), where $n(s)$ is given by

$$n(s) = \frac{1}{\pi\sqrt{s\,(N-s)}}. \tag{4}$$

According to this equation the tail length distribution is bimodal and symmetric: many conformations with short tails ($0 < s < 0.1N$), many conformations with long tails ($0.9N < s < N$), and relatively few conformations with intermediate tail length. Equation (4) was verified for a single off-lattice model chain[33] and for a lattice chain interacting with the surface with potentials having different widths.[34]

Equation (4) is normalized to unity: the integral over $n(s)$ from 0 to N is 1, which means that the number of tails is exactly 1: each conformation of a grafted continuum chain has precisely one tail, because the probability that the end point returns to *exactly* $z = 0$ is zero. We shall see that Eq. (4) is also a good approximation for the lattice model, but there is a minor (yet relevant) difference: the probability that the last segment ends up in the region $0 < z < 1$ (and thus is a train segment) is not zero. Conformations with the last segment in the first layer have no tail, so the number of tails (which we denote as n_0, see also the Appendix) is smaller than 1 in SCF, the more so for small N. In the lattice model n_0 is given by

$$n_0 = \sum_{s=1}^{N-1} n(s). \tag{5}$$

In order to compare the SCF results with Eq. (4), we normalize all profiles to unity: we use the probability $P(s) = n(s)/n_0$.

We are again interested in how $P(s)$ develops when we vary the concentration φ of the floating chains from 0 to 1. Figure 4 shows $P(s)$ profiles for the probe chain ($N = 1000$) at six bulk concentrations φ of the floating chains, for $\Delta\chi_s = 0$ (a), $\Delta\chi_s = 1$ (b), $\Delta\chi_s = -1$ (c). All data were obtained from SCF, but for comparison the analytical profile according to Eq. (4) is also shown. It is clear that for critical interactions between segments and surface ($\Delta\chi_s = 0$, Fig. 4(a)) there is absolutely no effect of the concentration φ, and that Eq. (4), which was derived for a single Gaussian chain, is an excellent approximation for the tail length distribution of a grafted chain at any concentration. This is in perfect agreement with the horizontal line for critical conditions in Figs. 3(a) and 3(b) (and in several of the following figures).

Therefore, the conformations of the probe chain in the melt can be divided in different populations, independent of surface interactions. There is a population with short tails ($s < 0.1N$), and a population with long tails ($0.9N < s$). The fraction of these two populations is close to 0.6. The remaining fraction of 0.4 has intermediate tail length.

Figures 4(b) and 4(c) show how these populations develop when the bulk concentration increases, for repulsion (Fig. 4(b)) and attraction (Fig. 4(c)). Starting from different conformations for repulsion (mushroom) and attraction (pancake) in dilute solution, the conformations acquire a universal character in the melt, independent of the surface interactions, and are described by Eq. (4).

In the analytical model for a Gaussian chain at critical conditions, the average tail length $\langle s\rangle$ is exactly $N/2$, and its dispersion $\delta(s) = [\langle s^2\rangle - \langle s\rangle^2]$ is $N^2/8$. In SCF this is approximately true, but there are minor corrections for short chains which vanish as $N^{-1/2}$. For more detail we refer to the Appendix.

VI. TRAIN FRACTION AND LOOP SIZE

Figure 5(a) shows how the train fraction ν of the probe chain (i.e., the fraction of chain segments in contact with the surface) develops when the concentration φ of the floating chains is increased from 0 to 1. This figure is for two chain lengths ($N = 50$ and 1000) and three values of the segment-surface interaction ($\Delta\chi_s = -1$, 0, 1). As before, we start with the data for $\varphi = 0$. For attraction, where the probe chain lies nearly flat (pancake), ν is of order unity and nearly independent of N. The SCF data are 0.919 ($N = 50$) and 0.728 ($N = 1000$) for $\Delta\chi_s = -1$.

For critical and repulsive (mushroom) conditions we have again analytical forms derived for a single end-attached chain:[32]

$$\nu = \frac{10}{\sqrt{6\pi N}}\left(1 - \frac{1}{\sqrt{6N/\pi}}\right) \quad \text{(critical)}, \tag{6a}$$

$$\nu = \frac{1}{N(1 - e^{-\Delta\chi_s})} \quad \text{(repulsion)}. \tag{6b}$$

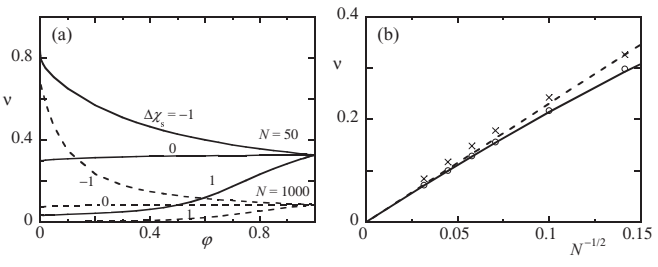

FIG. 5. (a) SCF results for the train fraction ν of the grafted chain as a function of φ, for $N = 50$ (solid curves) and $N = 1000$ (dashed), for critical conditions ($\Delta\chi_s = 0$, nearly horizontal curves), attraction ($\Delta\chi_s = -1$, decreasing curves), and repulsion ($\Delta\chi_s = 1$, increasing curves). (b) SCF data for the train fraction as a function of $1/\sqrt{N}$ at $\varphi = 0$, $\Delta\chi_s = 0$ (circles), and $\varphi = 1$, any $\Delta\chi_s$ (crosses). The solid curve is Eq. (6a) (full form), the dashed line is the leading term of Eq. (6a).

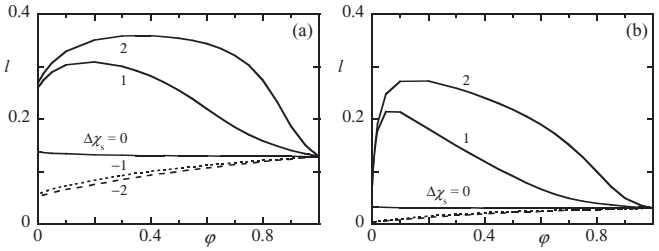

FIG. 6. Average relative loop length $l = L/N$ for $N = 50$ (a) and $N = 1000$ (b), for five values of $\Delta\chi_s$: −2, −1, 0, 1, 2.

Equation (6b) as such is not given in Ref. 32, but it follows from converting the extrapolation length as used in the continuum model to $\Delta\chi_s$.[25] Equations (6a) and (6b) perfectly describe the SCF data for a single chain. For critical conditions Eq. (6a) predicts $\nu = 0.262$ ($N = 50$), $\nu = 0.070$ ($N = 1000$), and SCF gives 0.298 and 0.071, respectively. For repulsion Eq. (6b) leads to $\nu = 0.022$ ($N = 50$), $\nu = 0.0016$ ($N = 1000$), nearly identical to the SCF data.

As we saw in Fig. 3 for ζ_1 and its dispersion $\delta(\zeta)$, with increasing φ the attraction and repulsion curves converge to a value in the melt ($\varphi = 1$) which is quite close to that of an isolated chain at critical conditions ($\Delta\chi_s = 0$).

Figure 5(b) gives the SCF values of ν for a single chain at critical conditions ($\varphi = 0$) and of the probe chain in the melt as a function of $1/\sqrt{N}$, and compares these with Eq. (6a). For $\varphi = 0$ (circles) there is excellent agreement with the full form of Eq. (6a) (solid curve). The melt data (crosses) are better described by only the leading term of Eq. (6a).

As a last characteristic of the probe chain, we show in Figs. 6 and 7 some selected data for the relative average loop length $l = L/N$ of the probe chain, where $L = \langle s \rangle$ is the average loop length. Figure 6 gives l as a function of the concentration φ for $N = 50$ (Fig. 6(a)) and $N = 1000$ (Fig. 6(b)). In both diagrams results are given for repulsion ($\Delta\chi_s = 2$ and 1), critical conditions ($\Delta\chi_s = 0$), and attraction ($\Delta\chi_s = -1$ and -2).

Like in the previous figures, we see the familiar (nearly) horizontal line for critical conditions. The level of this horizontal line is the only feature of Fig. 6 for which we have an analytical description. At critical conditions the loop-size distribution of a single chain is approximately given by[34,35] $n(s) \sim s^{-3/2}$, where $n(s)$ is the number of loops with size s. The average loop length $L = \langle s \rangle$, found from $\int sn(s)ds / \int n(s)ds$ with integration limits $s = 0$ and $s = N$, is $L = N^{1/2}$, and therefore the relative loop length is $l = N^{-1/2}$. This gives $l = 0.141$ for $N = 50$ and 0.032 for $N = 1000$. The SCF results for $N = 50$ are 0.137 ($\varphi = 0$) and 0.129 ($\varphi = 1$), and those for $N = 1000$ are 0.034 ($\varphi = 0$) and 0.031 ($\varphi = 1$). Hence, $n(s) \sim s^{-3/2}$ is a reasonable approximation for the SCF data for critical conditions (as also demonstrated from analyzing the SCF $n(s)$ profiles, not shown here). The same feature was demonstrated for lattice chains adsorbing with potentials with different widths.[34] For the attractive case the isolated chain ($\varphi = 0$) lies nearly flat: most segments are in trains (see also Fig. 5(a)) and the average loop length is small: L is independent of N and $\Delta\chi_s$, and consequently $l \sim N^{-1}$. As φ increases, we see a smooth increase of l towards the critical value at $\varphi = 1$, with hardly any effect of $\Delta\chi_s$.

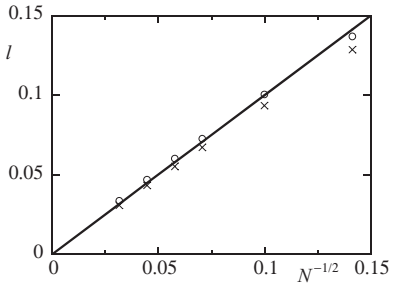

FIG. 7. Average relative loop length l for a single chain at critical conditions (circles) and for the probe chain in the melt (crosses) as a function of $1/\sqrt{N}$. The solid line is $l = 1/\sqrt{N}$.

For repulsion we find in Fig. 6 a non-monotonic behavior of the relative loop length as a function of concentration. For $\varphi = 0$, $l \approx 2\ N^{-1/2}$, which is twice the critical value. For $\varphi = 1$, l approaches the critical value $N^{-1/2}$, as expected. However, for intermediate φ the relative loop length l passes through a maximum. This non-monotonic behavior of the loop length is related to the tail distribution. At repulsive conditions a single grafted chain at $\varphi = 0$ has no long loops because almost all units are in tails. With increasing φ the tail length decreases and long loops appear. Yet, also for the loop length at high φ the convergence to critical conditions holds: for all the properties of the probe chain our central concept (melt equivalent to an isolated critical chain) is valid.

The chain-length dependence of the relative loop length l for a single chain at critical conditions ($\varphi = 0$) and the probe chain in the melt ($\varphi = 1$) are shown in Fig. 7. It is again clear that the two situations are nearly equivalent. Moreover, l is accurately given by $l = 1/\sqrt{N}$.

VII. RESULTS FOR MORE REFINED MODELS

All the SCF data presented so far are for a simple 6-choice lattice ($R = \sqrt{(N/6)}$, $\chi_{sc} = \ln(5/6)$) where immediate step reversals are allowed. In order to see whether the equivalence of single-chain conformations at critical conditions ($\varphi = 0$) and conformations in the melt ($\varphi = 1$) also holds for a slightly more sophisticated model, we did some SCF calculations for a 5-choice lattice ($R = \sqrt{(N/4)}$, $\chi_{sc} = \ln(4/5)$), where immediate step reversals are forbidden. The results are qualitatively the same. Even quantitatively they are very close, provided we take the different R and different χ_{sc} into account.

For example, the first moment $\zeta_1 = z_1/2R$ of the end-point distribution as a function of the concentration φ of the floating chains for 5-choice is nearly the same as Fig. 3(a) for 6-choice. We do not give the 5-choice figure, and restrict ourselves to comparing some characteristics. For $\varphi = 0$ and strong repulsion we found $\zeta_1 = 0.866$ in Fig. 3(a), and the 5-choice value is 0.927. More important is the critical value, where in Fig. 3(a) $\zeta_1 = 0.564$ for both $\varphi = 0$ and $\varphi = 1$. From the 5-choice data we have 0.597, again independent of φ, and we see the familiar horizontal line for critical conditions also for the 5-choice model. We, therefore, trust that our basic assumption is valid, not only for model lattice chains but also for real chains.

Both in a six-choice and in a five-choice lattice the radius of gyration R of a single chain is proportional to $\sqrt{N}$: there is no chain swelling because in an extremely dilute solution the field is zero and the internal excluded volume is absent. In a more sophisticated SCF model[36] it is possible to account for this excluded volume on the Flory level, using a spherical lattice for the grafted chain. Now a single chain at $\varphi = 0$ is swollen and R scales more or less like the Flory limit $N^{0.6}$. However, in the melt the probe chain becomes again ideal because the excluded-volume interactions are screened. The result is that for such a Flory chain at critical conditions we do not find a horizontal line for z_1 as a function of the concentration φ, but a decreasing curve.

Let us compare not the scaled end-point position ζ_1, but the unscaled z_1, where we consider the three values (attraction, critical, repulsion) for a single grafted chain ($\varphi = 0$) and the one value for the probe chain in the melt. For the simple 6-choice lattice ($N = 1000$) these values are 1.84, 14.64, 22.88 ($\varphi = 0$), and 14.64 ($\varphi = 1$). For the 5-choice data we have 3.17, 18.88, 29.31 ($\varphi = 0$), and 18.88 ($\varphi = 1$). These values are somewhat higher than for 6-choice because a 5-choice chain is more extended since immediate step reversals are forbidden. For a Flory chain we find 4.04, 24.3, 30.5 ($\varphi = 0$), and 15.7 ($\varphi = 1$). Here, we see the effect that z_1 of a swollen chain at $\varphi = 0$ is higher than that of a screened chain in the melt (which has about the same z_1 as in a simple 6-choice lattice), but the feature that in the melt the value of the segment-surface interaction does not play any role is also valid for a Flory chain.

VIII. DISCUSSION

The most important result of this paper is that a grafted chain in the melt has about the same conformations as a single chain under critical conditions, at least for the 6-choice and 5-choice lattice without intramolecular excluded volume, and that these melt conformations are independent of the polymer-surface interactions. For a Flory chain with internal excluded volume a single chain is swollen, but in the melt interactions are screened and the conformations are again (half) Gaussian; also for a Flory chain there is no effect of the adsorption energy in the melt. Although we analyzed only the properties of the grafted probe chain, it is clear that the conformations of all chains in the surface region of the melt are close to those of an appropriate single chain in critical conditions, provided that one end of the single chain is fixed at the same point as a chain in the melt.

We now discuss why in the melt critical conformations are realized at *any* polymer/substrate interaction. To answer this question we look again at Fig. 1(b), where concentration profiles of the floating chains are shown at critical conditions ($\Delta\chi_s = 0$). All profiles are flat at any concentration, from a dilute solution to the melt. There is a well-known principle formulated by Flory[22] about the possibility to fill a volume in the bulk with constant density by polymer coils in random Gaussian conformations. We can generalize this statement to the interfacial properties: to fill uniformly the volume in the surface region we need polymer chains in critical conformations. In other words, uniform filling in the melt needs critical (half Gaussian) conformations.

There is a thermodynamic explanation of this effect: to compensate the loss of entropy close to a substrate a single polymer chain needs weak adsorption. At critical interactions the entropic and enthalpic effects compensate each other and the surface becomes "invisible." It corresponds to reflecting boundary conditions.

To understand why the conformations of a polymer chain in the melt do not depend on polymer/substrate interactions, we first have to consider the situation in a dilute solution where each polymer/substrate contact is accompanied by the loss of a solvent/substrate contact. The difference of the free energies polymer/substrate and solvent/substrate defines what conformations – pancake or mushroom – are realized in a dilute solution. At critical conditions this free energy difference is zero. The situation in the melt is similar: each polymer/substrate contact is accompanied by the loss of another polymer/substrate contact and again there is no effect on the free energy.

Another question is the relation between lattice and off-lattice model chains. Both these models are coarse-grained, and can be used as models for non-crystalline, amorphous polymers. A segment of a lattice model chain can be associated with the Kuhn segment of a real flexible polymer chain. Off-lattice models are more detailed: the repeating unit is similar to a monomer unit of flexible polymers. This difference leads to different monomer density profiles in melt for these two models. Off-lattice models as well as atomistic simulation of amorphous polymers in the melt demonstrate three or four oscillations of monomer density profiles near a solid substrate. These oscillations, associated with packing effects, involve 3-4 layers and disappear when the distance from the substrate is of the order of a Kuhn segment. The relation between coarse-grained polymer models and the chemically realistic description of a polymer melt on the atomic scale was discussed in detail by Muller *et al.*[9] Note that the weak dependence of the average characteristics on the polymer/substrate interaction obtained in some off-lattice computer simulations[17] can be explained by the difficulty to reach a fully condensed melt with $\varphi = 1$. In SCF calculations this problem is absent.

There are also oscillations in the SCF model for the melt, but not in the density: this imposed at $\varphi = 1$. Now the field $u(z)$ oscillates in the melt, for purely space-filling reasons. Nevertheless, the field in the melt is close to that for a single chain at critical conditions, see Fig. 8.

We first discuss the consequences of the critical step profile of Fig. 8. Since the seminal work of DiMarzio and Rubin[37] it is known that in such a step profile the end-point distribution $\varphi_e(z)$ for free (non-grafted) chains at (very) low φ is homogeneous. For infinitely long chains the overall profile $\varphi_o(z)$ is homogeneous for $z > 1$, but it shows a dip (in this case by a factor of 5/6) in the first layer, see Fig. 2(c). For an end-grafted chain (the probe chain) the distribution cannot be homogeneous (it is a half-Gaussian, see Fig. 2(c)), but the dip in the overall profile remains, see again Fig. 2(c).

For the melt we have (weak) oscillations in the field $u(z)$. Now the overall concentration of the floating chains is

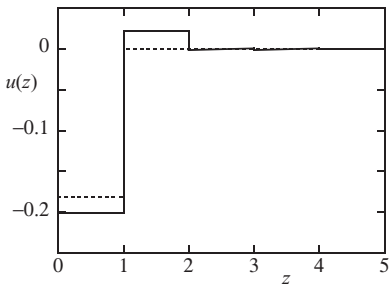

FIG. 8. The potential profile $u(z)$ for critical conditions and $N = 50$ (a step function with $u = \ln(5/6) = -0.182$ in the train layer and $u = 0$ elsewhere, dotted profile) and in the melt (where u oscillates due to space filling). The first 5 values for the melt profile are -0.201, 0.022, -0.0018, 0.0004, 0.0001.

homogeneous ($\varphi(z) = 1$ for any z by definition) and the surface layer is slightly enriched with end points. The same effect is seen for the probe chain, which explains the slight upward jump for the end-point profile in Fig. 2(d).

The (small) difference in the u-profiles in Fig. 8 gives rise to (slightly) different properties for $\varphi = 0$ (critical) and $\varphi = 1$, as shown in several figures in this paper. We give one more illustration in Fig. 9: floating-chain profiles $\varphi(z)/\varphi$ for three concentrations and two chain lengths. The concentrations φ are 10^{-10}, 0.1, and 1; the chain lengths are $N = 50$ (Fig. 9(a)) and $N = 1000$ (Fig. 9(b)).

The melt limit $\varphi(z) = \varphi = 1$ is clear in both diagrams (horizontal line). In the other extreme ($\varphi \to 0$) the DiMarzio-Rubin limit would be $\varphi_1 = (5/6)\varphi = 0.833\varphi$, $\varphi_z = \varphi$ for $z > 1$. This limit is not quite reached in Fig. 9, not even for $N = 1000$ (Fig. 9(b)) where for $z > 1$ there is still a (small) excess of polymer over a relatively wide region. However, from comparing $N = 50$ (Fig. 9(a)) and $N = 1000$ (Fig. 9(b)) one can see that that for still higher N the profile approaches this limit. For an intermediate concentration ($\varphi = 0.1$) the profile is also intermediate, with a smaller dip for $z = 0.5$ and a weaker excess (over just a few layers) for $z > 1$.

We can conclude that a coarse-grained lattice model is more primitive and has a smaller resolution in comparison with off-lattice models. As was pointed by Muller *et al.*[9] "in a dense polymer melt the screening length ξ becomes comparable to the statistical segment length, and the discrete molecular structure of a real polymer chain becomes important on the length scale ξ. In this region the physical properties of the interface are not completely described by coarse-grained models. Molecular stiffness, shape of the repeating units, and their packing exert a pronounced influence on the properties of the narrow polymer-solid interface". Our paper is dedicated to large-scale equilibrium properties of the interface in the melt as well as in concentrated solutions, where the typical length exceeds the statistical segment length.

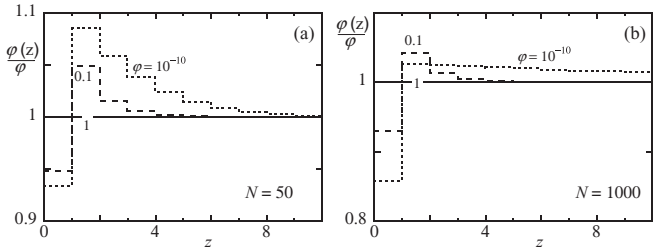

FIG. 9. Relative profiles $\varphi(z)/\varphi$ of the floating chains, for $\Delta\chi_s = 0$ and $\varphi = 10^{-10}$, 0.1, and 1. In Fig. 9(a) the chain length is 50, in (b) it is 1000.

IX. CONCLUDING REMARKS

In this paper we focus on the conformations of a probe chain grafted by one end to a solid surface in a sea of floating chains with varying concentrations. The chain length, flexibility, and potential interactions between units as well as the polymer-surface interactions are identical for probe chain and floating chains. In several of the figures presented in this paper, we saw that the equilibrium properties of a probe chain in the melt are very close to those for a single grafted chain at critical conditions, for which an analytical description is available. Recall that critical conditions correspond to weak adsorption. It was shown also that all equilibrium properties of a probe grafted chain in melt do not depend on the polymer-surface interactions; these interactions were varied from strong repulsion to strong adsorption. When the polymer-surface interactions are fixed and set equal to the critical adsorption energy, all equilibrium properties of a probe chain do not change with the concentration of the floating chains, from zero concentration to the melt.

We note in conclusion that the equivalence between melt conformations and critical Gaussian conformations is not strictly valid: both the Flory hypothesis for the bulk and the Silberberg generalization to the surface region are useful concepts but they are only approximate. In a seminal paper by Muthukumar and Edwards,[38] it was shown that the statistical segment size depends on the polymer concentration. So the isolated ideal critical chain is not quite the same as the bulk chain in the melt. Other papers[39–41] also showed that chains in the melt are not strictly Gaussian.

Finally, we described the critical conformations of a Gaussian chain by the Edwards equation with a De Gennes boundary condition. Alternative boundary conditions which implement the notion that the polymer density in the solid boundary vanishes[42,43] have been considered. Then there are deviations for short chains, but simple analytical solutions are not easily found.

APPENDIX: CHAIN-LENGTH CORRECTIONS FOR THE AVERAGE TAIL LENGTH AND ITS DISPERSION UNDER CRITICAL CONDITIONS

As mentioned in Sec. V, in the analytical model for a Gaussian chain under critical conditions each conformation has as exactly one tail ($n_0 = 1$), the average tail length $\langle s \rangle$ is exactly $N/2$, and its dispersion $\delta(s)$ is $N^2/8$. In SCF this is approximately true, but there are minor corrections for short chains, which we analyze in this appendix.

We define the following moments for the numerical SCF distribution $n(s)$:

$$n_0 = \sum_{s=1}^{N-1} n(s), \tag{A1a}$$

$$n_1 = \sum_{s=1}^{N-1} sn(s), \tag{A1b}$$

$$n_2 = \sum_{s=1}^{N-1} s^2 n(s), \tag{A1c}$$

where n_0 is the number of tails. Even when we use Eq. (4) for $n(s)$, we find now $n_0 < 1$. It can be shown that substituting Eq. (A1) into Eq. (4) gives the following (empirical) analytical approximations:

$$n_0 = 1 - \frac{a_0}{\sqrt{N}}, \tag{A2a}$$

$$n_1 = \frac{N}{2}\left(1 - \frac{a_1}{\sqrt{N}}\right), \tag{A2b}$$

$$n_2 = \frac{3N^2}{8}\left(1 - \frac{a_2}{\sqrt{N}}\right), \tag{A2c}$$

where $a_0 = a_1 = 0.93$ and $a_2 = 1.23$ when Eq. (4) is valid. In the pure continuum model $a_0 = a_1 = a_2 = 0$. For the SCF results we find that Eq. (A2) applies with slightly different numerical constants ($a_0 = 1.35$, $a_1 = 1.15$, $a_2 = 1.5$). This means that Eq. (4) is not strictly valid in SCF, although it remains a good approximation and a valuable reference for interpreting the numerical data.

From the moments n_0, n_1, n_2, we obtain the average relative tail length $t = \langle s\rangle/N$ and its dispersion $\delta(t) = [\langle s^2\rangle - \langle s\rangle^2]/N^2$ as

$$t = \frac{n_1}{Nn_0}, \tag{A3a}$$

$$\delta(t) = \frac{1}{N^2}\left(\frac{n_2}{n_0} - \left(\frac{n_1}{n_0}\right)^2\right). \tag{A3b}$$

If Eq. (4) applies, the result is $t = 1/2$ and $\delta(t) = (1 - 3.69/\sqrt{N})/8$. For the SCF data, where Eq. (4) is not strictly valid, we shall find (very) minor deviations in both t and $\delta(t)$.

Figure 10(a) shows the SCF results for the average relative tail length $t = \langle s\rangle/N$ as a function of $1/\sqrt{N}$ for a single chain ($\varphi = 0$) at critical conditions and for the probe chain in the melt ($\varphi = 1$), for the range $N = 50$ to 1000. The theoretical result from Eq. (4) is $t = 1/2$, which is nearly exactly true for the SCF data in the melt. For $\varphi = 0$ there are (very) minor deviations ($t = 0.511$ for $N = 50$), which implies that Eq. (4) is not strictly obeyed, although it is still a very good approximation. The small deviations occur because the numerical constants a_0 and a_1 in Eq. (7) (which are the same when Eq. (4) applies), are slightly different in the SCF results. The straight line for critical conditions in Fig. 5(a) is $t = (1 + 0.2/\sqrt{N})/2$, where the numerical constant is $a_0 - a_1 = 1.35 - 1.15$.

In Fig. 10(b) $\delta(t)$, the dispersion of t, is shown. Now there is hardly any difference between critical conditions and the melt. For long chains $\delta(t)$ approaches the theoretical value 1/8 as $1/\sqrt{N}$. When Eq. (4) would strictly apply, we would expect $\delta(t) = (1 - 3.69/\sqrt{N})/8$. In Fig. 5(b) the straight line for SCF is drawn according to $(1 - 1.25/\sqrt{N})/8$ for both $\varphi = 0$ and $\varphi = 1$; the numerical constant 1.25 follows directly from the SCF values for a_0, a_1, a_2 as given above.

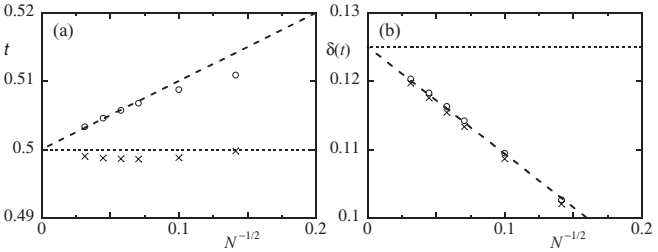

FIG. 10. Average relative tail length $t = \langle s\rangle/N$ (a) and its dispersion $\delta(t)$ (b) as a function of $1/\sqrt{N}$, for critical conditions and $\varphi = 0$ (circles) and $\varphi = 1$ (crosses). The theoretical limits $t = 1/2$ (a) and $\delta(t) = 1/8$ (b) are indicated as the horizontal dotted lines.

[1]L. Yelash, P. Virnau, K. Binder, and W. Paul, Phys. Rev. E **82**, 050801 (2010).
[2]R. Hentschke, B. L. Schurmann, and J. P. Rabe, J. Chem. Phys. **96**, 6213 (1992).
[3]K. F. Mansfield and D. N. Theodorou, Macromolecules **22**, 3143 (1989); **23**, 4430 (1990); **24**, 4295 (1991); **24**, 6283 (1991).
[4]G. D. Smith, D. Y. Yoon, and R. L. Jaffe, Macromolecules **25**, 7011 (1992).
[5]K. Ch. Daoulas, V. A. Harmandaris, and V. G. Mavrantzas, Macromolecules **38**, 5780 (2005).
[6]Y. N. Pandey and M. Doxastakis, J. Chem. Phys. **136**, 094901 (2012).
[7]J. M. H. M. Scheutjens and G. J. Fleer, J. Phys. Chem. **83**, 1619 (1979).
[8]G. J. Fleer, M. A. Cohen Stuart, J. M. H. M. Scheutjens, T. Cosgrove, and B. Vincent, *Polymers at Interfaces* (Chapman and Hall, London 1993).
[9]M. Muller, B. Steinmuller, K. Ch. Daoulas, A. Ramirez-Hernandez, and J. J. de Pablo, Phys. Chem. Chem. Phys. **13**, 10491 (2011).
[10]D. N. Theodorou, Macromolecules **21**, 1400 (1988); **22**, 4578 (1989); **22**, 4589 (1989).
[11]I. Bitsanis and G. Hadziioannou, J. Chem. Phys. **92**, 3827 (1990).
[12]I. Bitsanis and G. ten Brinke, J. Chem. Phys. **99**, 3100 (1993).
[13]D. Smith, D. Bedrov, and O. Borodin, Phys. Rev. Lett. **90**, 226103 (2003).
[14]M. S. Ozmusul, C. R. Picu, S. S. Sternstein, and S. K. Kumar, Macromolecules **38**, 4495 (2005).
[15]M. Vacatello, Macromolecules **35**, 8191 (2002); **34**, 1946 (2001).
[16]J. S. Meth and S. R. Lustig, Polymer **51**, 4259 (2010).
[17]A. de Virgiliis, A. Milchev, V. G. Rostiashvili, and T. A. Vilgis, Eur. Phys. J. E **35**, 97 (2012).
[18]D. Wu, G. H. Fredrickson, J.-P. Carton, A. Ajdari, and L. Leibler, J. Polym. Sci. B **33**, 2373 (1995).
[19]J. B. Avalos and A. Johner, Faraday Discuss. **98**, 111 (1994).
[20]A. Silberberg, J. Colloid Interface Sci. **90**, 86 (1982); **125**, 14 (1988).
[21]E. Eisenriegler, K. Kremer, and K. Binder, J. Chem. Phys. **77**, 6296 (1982).
[22]P. J. Flory, *Principles of Polymer Chemistry* (Cornell University Press, Ithaca, 1953).
[23]S. F. Edwards, Proc. Phys. Soc. **85**, 613 (1965); **88**, 265 (1966).
[24]M. Doi and S. F. Edwards, *The Theory of Polymer Dynamics* (Clarendon Press-Oxford, 1986).
[25]G. J. Fleer and A. M. Skvortsov, J. Chem. Phys. **136**, 134707 (2012).
[26]C. M. Wijmans and F. A. M. Leermakers, Colloids Surf., A Physicochemical and Engineering Aspects **86**, 61 (1994).
[27]P. J. de Gennes, *Scaling Concepts in Polymer Physics* (Cornell University Press, Itheca, 1979).
[28]G. J. Fleer, A. M. Skvortsov, and R. Tuinier, Macromolecules **36**, 7857 (2003).
[29]G. J. Fleer, J. van Male, and A. Johner, Macromolecules **32**, 825 (1999).
[30]H. N. W. Lekkerkerker and R. Tuinier, *Colloids and the Depletion Interaction* (Springer, 2011).
[31]A. A. Gorbunov and A. M. Skvortsov, Adv. Colloid Interface Sci. **62**, 31 (1995).
[32]A. A. Gorbunov, A. M. Skvortsov, J. van Male, and G. J. Fleer, J. Chem. Phys. **114**, 5366 (2001).

[33]S. Bhattacharya, V. G. Rostiashvili, A. Milchev, and T. A. Vilgis, Phys. Rev. E **79**, 030802 (2009).
[34]L. I. Klushin, A. A. Polotsky, H.-P. Hsu, D. A. Markelov, K. Binder, and A. M. Skvortsov, Phys. Rev. E **87**, 022604 (2013).
[35]C. A. J. Hoeve, E. A. DiMarzio, and P. Peyser, J. Chem. Phys. **42**, 2558 (1965).
[36]B. R. Postmus, F. A. M. Leermakers, and M. A. Cohen Stuart, Langmuir **24**, 1930 (2008).
[37]E. A. DiMarzio and R. J. Rubin, J. Chem. Phys. **55**, 4318 (1971).
[38]M. Muthukumar and S. F. Edwards, J. Chem. Phys. **76**, 2720 (1982).
[39]P. Beckrich, A. Johner, A. N. Semenov, S. P. Obukhov, H. Benoit, and J. P. Wittmer, Macromolecules **40**, 3805 (2007).
[40]A. Cavallo, M. Muller, J. P. Wittmer, A. Johner, and K. Binder, J. Phys. Condens. Matter **17**, S1697 (2005).
[41]J. P. Wittmer, A. Cavallo, H. Xu, J. E. Zabel, P. Polinska, N. Schulmann, H. Meyer, J. Farago, A. Johner, S. P. Obukhov, and J. Baschnagel, J. Stat. Phys. **145**, 1017 (2011).
[42]I. Y. Erukhimovich, A. Johner, and J. F. Joanny, Eur. Phys. J. E **27**, 435 (2008).
[43]M. W. Matsen, J. U. Kim, and A. E. Likhtmann, Eur. Phys. J. E **29**, 107 (2009).